Thin Solid Films xxx (2016) xxx–xxx

Contents lists available at ScienceDirect

Thin Solid Films

journal homepage: www.elsevier.com/locate/tsf

Effective medium approximation of ellipsometric response from random surface roughness simulated by finite-element method

B. Fodor [a,b,*], P. Kozma [a], S. Burger [c], M. Fried [a,d], P. Petrik [a,d]

[a] Institute for Technical Physics and Materials Science (MFA), Centre for Energy Research of the Hungarian Academy of Sciences, Konkoly Thege út 29-33, H-1121 Budapest, Hungary
[b] Doctoral School of Molecular- and Nanotechnologies, Faculty of Science, University of Pécs, Ifjúság útja 6, H-7624 Pécs, Hungary
[c] Zuse Institute Berlin (ZIB), Takustrasse 7, D-14195 Berlin, Germany
[d] Doctoral School of Molecular- and Nanotechnologies, Faculty of Information Technology, University of Pannonia, Egyetem u. 10, Veszprém H-8200, Hungary

A R T I C L E I N F O

Article history:
Received 2 September 2015
Received in revised form 27 January 2016
Accepted 28 January 2016
Available online xxxx

Keywords:
Ellipsometry
Surface roughness
Effective medium approximation
Finite-element method
Root mean square height
Correlation length

A B S T R A C T

We used numerical simulations based on the finite-element method (FEM) to calculate both the amplitude and phase information of the scattered electric field from random rough surfaces, which can be directly compared to ellipsometric measurements and effective medium approximation (EMA) calculations. FEM can serve as an exploration tool for the relationship between the thickness of the surface roughness evaluated by Bruggeman EMA and the morphological parameters of the surface, such as the root mean square height, the lateral auto-correlation length, and the typical average slope. These investigations are of high interest in case of poly-crystalline and amorphous materials. The paper focuses on the simulations of rough Si surfaces. The ellipsometric calculations from FEM and EMA simulations match for wavelengths of illumination much shorter than the typical feature size of the surface. Furthermore, for these cases, the correlation between the EMA thickness and the root mean square height of the roughness for a given auto-correlation length is quadratic, rather than linear, which is in good agreement with experimental measurements and analytical calculations presented in recent reports.

1. Introduction

Characterizing surface roughness with ellipsometry has become a routine practice since the birth of spectroscopic ellipsometry because of its fast, non-destructive, and in-line capabilities. The most widely used models describe the surface roughness with an effective medium approximation (EMA), i.e. the surface roughness is considered a homogeneous layer with an effective dielectric function mixed from the dielectric functions of the two media separating the rough interface. A good review about the relationship between surface morphology and EMA roughness can be found in Ref. [1]. Many experimental comparisons have been made between the EMA measured by ellipsometry and the morphology measured by atomic-force microscopy (AFM) for different Si samples: wet etched and thermally annealed Si [2], CVD deposited poly-Si [3,4], and poly-Si-on-oxide [5], as well as for in-situ growth of amorphous hydrogenated Si [6] and CVD deposited microcrystalline-Si on amorphous Si [7]. These works all concluded at a positive linear relationship between EMA roughness and AFM root mean square height, but all with different linear parameter values (slope and offset). One study even showed a negative correlation [8], stating that AFM measurements indicate an increase in root mean square height while ellipsometry suggests a smoothening of roughness. To better grasp the kaleidoscope of these different results, the present study simulates the ellipsometric response of a large number of random Si surfaces with well-defined root mean square heights and correlation lengths. The numerical simulations have been made by finite-element methods (FEM). FEM is a numerical technique to find approximate solutions of partial differential equations. Optical FEM is based directly on the linear Maxwell's equations in frequency domain. Computation of the electric (and the magnetic) field amplitudes are solved on a polygonal mesh, typically triangular, with piecewise-polynomial interpolation between the mesh points. Arbitrary geometrical objects can be defined with permittivity and permeability values assigned to each object (more specifically, assigned to the mesh points approximating the object). A summary of the vast areas of interest of the optical FEM can be found in Ref. [9]. The ellipsometric simulations of the random rough surfaces may be considered in our case as the "measured" samples and the effective medium roughness as the model to be fitted. This approach reveals many interesting effects concerning the relationship between the surface morphology and the thickness of the EMA roughness.

2. Model structures

Electromagnetic near fields resulting from plane wave illumination of silicon surfaces with roughness were simulated using the finite-

* Corresponding author at: Institute for Technical Physics and Materials Science (MFA), Centre for Energy Research of the Hungarian Academy of Sciences, Konkoly Thege út 29-33, H-1121 Budapest, Hungary.
E-mail address: fodor@mfa.kfki.hu (B. Fodor).

http://dx.doi.org/10.1016/j.tsf.2016.01.054
0040-6090/© 2016 Published by Elsevier B.V.

element solver JCMSuite (version 2.16). Specular reflection amplitudes (and intensities) were obtained from far field results computed in post-process as a spatial (discrete) Fourier spectrum. Although the Maxwell equations are solved as stationary wave solutions in frequency domain, from the complex scattered electric fields, both the amplitude and phase information can be obtained. As the electric fields of the incident plane waves polarized parallel (P) and perpendicular (S) to the plane of incidence in the finite-element simulations are defined with unit amplitudes, the ellipsometric complex ρ is obtained as the ratio of the reflected complex amplitudes of the P and S polarizations. The ellipsometric angles are defined in the usual way as $\Psi = tan^{-1}(\rho)$ and $\Delta = arg(\rho)$, where $tan\,\Psi$ is the amplitude ratio and Δ is the phase difference, respectively, of the complex reflection coefficients of P and S polarized light [10,11]. The spectra were simulated in a wavelength range from 200 to 1000 nm, in steps of 10 nm, for the angles of incidence of 65° and 75°. The near-field amplitudes had to be computed individually for each wave vector of the illumination, because of the optical dispersion of the Si material [12].

For computational reduction, the simulation domain was 2-dimensional, with a translational symmetry in the direction perpendicular to the plane of incidence. This very useful simplification is based on the assumption that cross-polarizations due to the anisotropic nature of the simulated surface (as opposed to a real randomly rough 2D surface) are negligible, as the surface features are much smaller than (λ). Furthermore, to eliminate scattering-like artifacts at the edge of the surface, periodic boundary conditions were used at these lateral sides of the computational domain. For the two remaining sides, transparent boundary condition was applied. The topographic points of the surface were generated with D. Bergström's Open Source MATLAB code [13] in such a way that the height distribution followed a Gaussian statistics. For visualization, a portion of the simulation mesh of a surface with a correlation length of 10 nm and a root mean square roughness of 2.5 nm is shown in Fig. 1a (left) with the height distribution histogram (right). An easy way to achieve such a height distribution is to convolute a predefined Gaussian filter on an uncorrelated (Gaussian) distribution of surface points generated by random numbers (i.e. white noise) [14]. The advantage of this approach is that the standard deviation of the uncorrelated distribution and of the Gaussian filter will be inherited and account for the root mean square height (R_{RMS}) and the correlation length (ξ) of the surface, respectively. Of course, due to the stochastic nature of the structure, small deviations will be present between the predefined standard deviations and the R_{RMS} values. To achieve adequate Gaussian statistics and diminish deviations from nominal values, the length of the surface to be simulated (L) was chosen such that $L/\xi \geq 500$. Additionally, L was at least 5 μm so that diffraction due to periodic boundary conditions would be negligible (parameter convergences as a function of L were studied). The simulated topographical parameters for ξ were 2.5, 5, 10, and 20 nm, while for the R_{RMS} were 0.5, 1, 1.5, 2.5, 3.5, 5, 7.5, 10, 15, and 20 nm. The combinations of all these parameter values are simulated, totaling in 40 points.

JCMSuite permits adaptive mesh refinement, i.e., after a pre-generated grid (following the curvature of the geometry), local grid refinements are applied as a function of the previously solved field amplitude gradients and a new refined mesh is calculated. These steps can be iterated to achieve adequate convergence and necessary precision. Faster convergences can be achieved when using higher FEM degrees. In our simulations, computational costs and ellipsometric angle convergences as a function of the refinement steps and the FEM

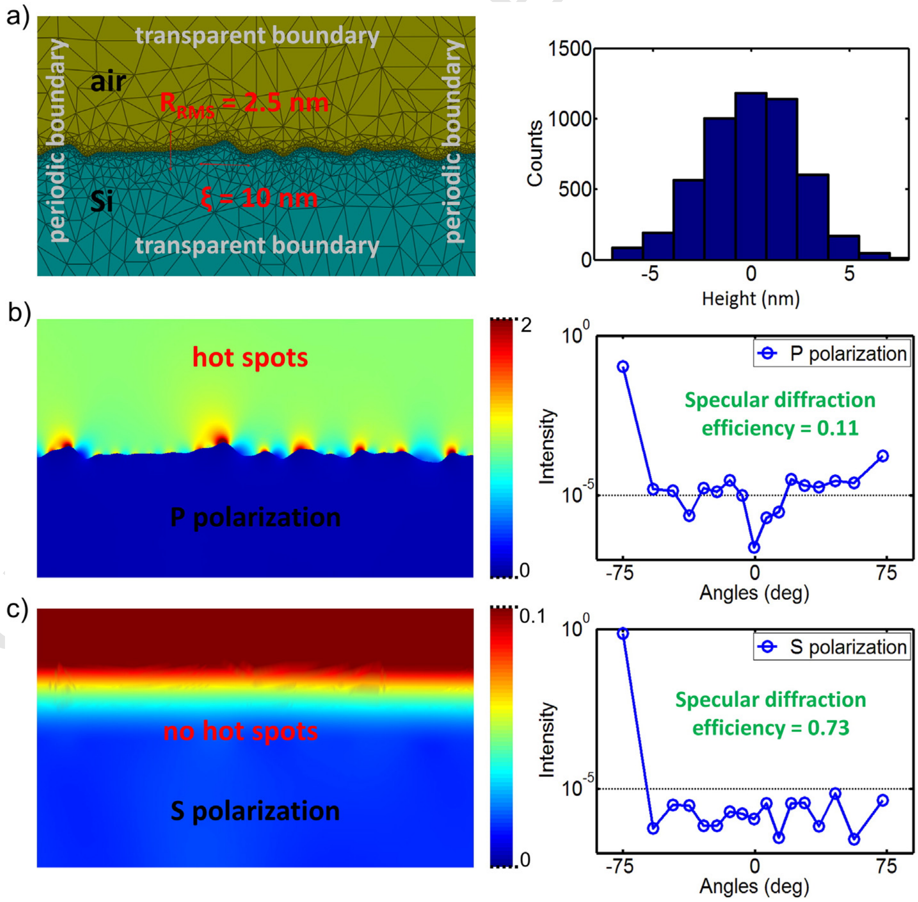

Fig. 1. Scattering simulation of one of the generated surface roughness for a plane wave incident at 75° at a wavelength of 600 nm. (a) Local grid structure after one refinement step (left) and the Gaussian distribution of surface heights (right). Near field intensity image and far field intensity angular distribution for (b) P polarization and for (c) S polarization (with −75° meaning the specular reflection).

Please cite this article as: B. Fodor, et al., Effective medium approximation of ellipsometric response from random surface roughness simulated by finite-element method, Thin Solid Films (2016), http://dx.doi.org/10.1016/j.tsf.2016.01.054

degree were also investigated. For the current morphologies (ξ and R_{RMS} are smaller than λ), a suitable compromise for computation costs was 1 refinement step and a FEM degree of 3, with which a Ψ convergence smaller than 10^{-2} and a Δ convergence smaller than 10^{-1} degree were achieved.

The FEM-simulated spectra were fitted with a planar thin layer structure using the transfer matrix method [11], where the surface roughness is considered to be an effective medium volumetrically composed of 50–50% of the two media [10, pp. 181–184]. D. E. Aspnes et al. concluded that the Bruggeman EMA showed the best fit results for the ellipsometric evaluations of various rough surfaces [15] and has been extensively used for such evaluations since then. The simplest single-layer EMA representing the surface roughness (see inset in Fig. 2a) has only one fit parameter, namely, its thickness value (d_{EMA}). The void is kept fixed at 50% as mentioned above, as the screening parameter as well, kept fixed at a value of 1/3, representing spherical inclusions in the EMA model. The fitting algorithm minimizes the mean square error (*MSE*), indicating the merit of fit. In our case, for one fitted parameter,

$$MSE = \sqrt{\frac{1}{N-2}\sum_{j=1}^{N}\left\{\left(\Psi_j^{FEM}-\Psi_j^{EMA}\right)^2+\left(\Delta_j^{FEM}-\Delta_j^{EMA}\right)^2\right\}},$$

where the superscripts '*FEM*' and '*EMA*' of Ψ and Δ indicate the FEM simulation values and the fitted EMA values, respectively, while *N* is the number of independently simulated spectral points.

3. Results and discussion

The small surface features cause high-intensity spots in near field around the sharp features of surface protrusions for the *P* polarization, which are not present for the *S* polarization (see left images of Fig. 1b and c, respectively, for plane wave illumination at an angle of incidence of 75° and a wavelength of 600 nm). The difference for the two polarizations is clearly accountable in the diffracted far field intensity values as well. The right-hand side images of Fig. 1b and c show the angular intensity distributions of the two polarizations. Although the ellipsometric angles were calculated solely from the 0th order (specular) diffracted amplitudes, it is interesting to note that apart from the specular intensity differences (diffraction efficiency of 0.11 for *P* polarization and 0.73 for *S* polarization), there is (generally) an order of magnitude difference in the higher order diffracted angles between the two polarizations. For cases where λ is much larger than the typical feature size of the surface roughness, non-specular scattering would be negligible for ellipsometric considerations and also EMA models are applicable. At wavelengths comparable to the typical feature size, scattering starts to dominate and EMA clearly fails to describe the roughness. To demonstrate this phenomenon, Fig. 2 shows the EMA-fitted spectra on simulations with an increasing R_{RMS} value (R_{RMS} = 1, 5, and 10 nm for Fig. 2a–c, respectively) for an identical ξ = 10 nm. For the R_{RMS} = 1 nm (d_{EMA} = 0.3 nm), an almost perfect match can be fitted, while for the R_{RMS} = 5 nm case (d_{EMA} = 6.7 nm), small deviations at the UV part of the spectra start to appear with an increase in the *MSE* value. Finally, for the R_{RMS} = 10 nm case (d_{EMA} = 24 nm), fitting on the whole spectra would be inappropriate, biasing the evaluated roughness; the fit shown in Fig. 2c was made in a wavelength range of 800–1000 nm only (*MSE* = 1), and the Ψ and Δ angles were generated (extrapolated) to the whole range to point out the huge deviations from the FEM simulations below λ = 600 nm. These deviations are more pronounced than what would be expected in case of a real measurement fitted with EMA models at these R_{RMS} values. The difference is probably because of the simplification of using 2D models. 3D simulations will be made in future studies to investigate these effects.

For the following discussion, only the simulations where the whole spectral range can be fitted with the EMA model (*MSE* < 3) are

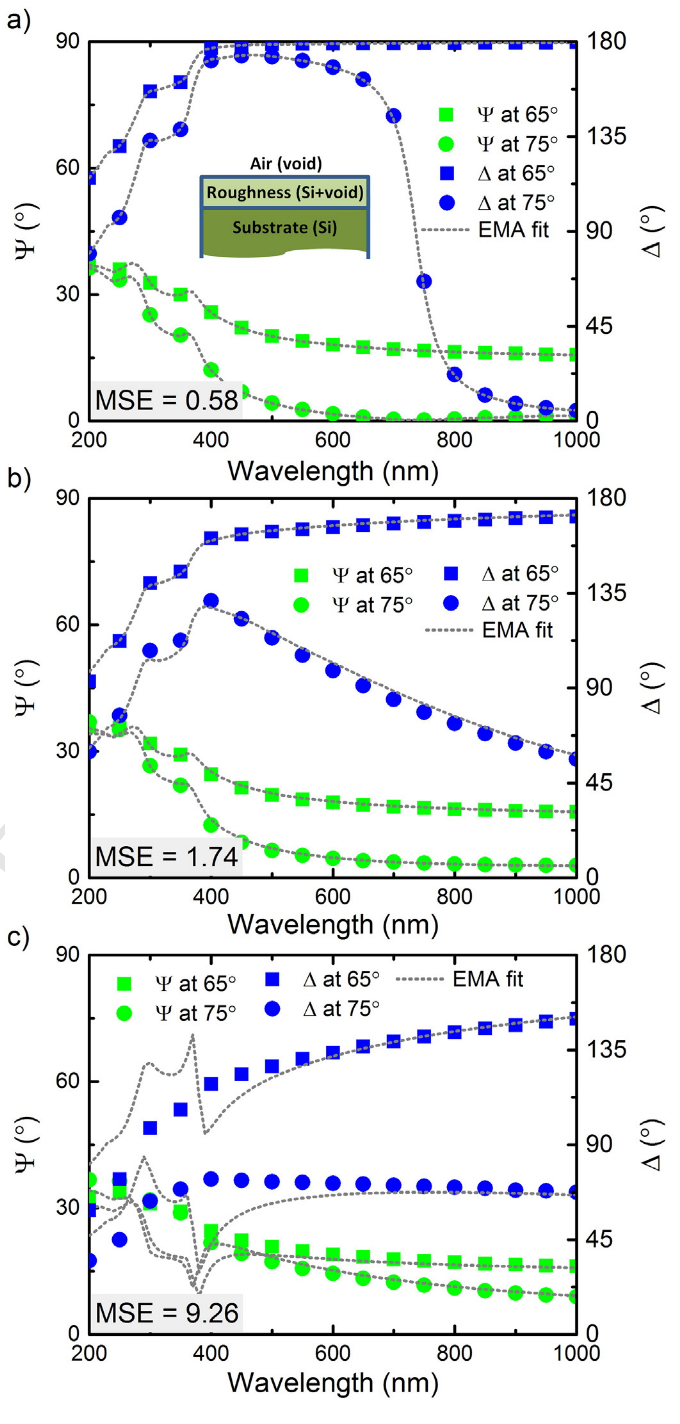

Fig. 2. FEM simulations of Ψ and Δ spectra fitted with an EMA surface roughness (see the model in the inset) of the samples with a nominal correlation length (ξ) of 10 nm and with a nominal root mean square roughness of (a) 1 nm, (b) 5 nm, and (c) 10 nm. Mean square errors (*MSE*) are also included in the graphs.

considered. Fig. 3 summarizes the dependence of d_{EMA} on the R_{RMS} and ξ values. The most conspicuous effect is that separate relations can be established between the d_{EMA} and the R_{RMS}, depending on ξ. Interestingly, quadratic relation fits are much more accurate than simple linear ones at these parameter ranges. Additionally, the different "curvatures" indicate that ellipsometry is more sensitive to sharper surface roughness features in the microscopic regime, i.e., for shorter ξ values, fitted d_{EMA} increases at a higher pace as a function of R_{RMS} than for longer ξ values. This effect agrees well with the conclusion made in Ref. [8] that ellipsometry is sensitive on roughness only on relatively short

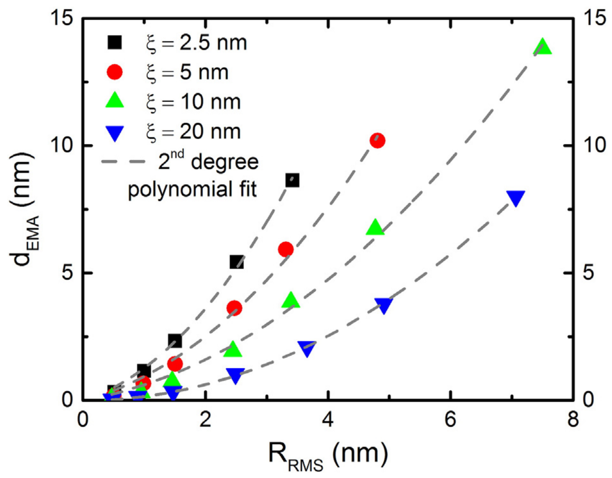

Fig. 3. Second degree polynomial correlation between the root mean square roughness (R_{RMS}) and the thickness of the effective medium roughness (d_{EMA}) for different correlation lengths (ξ).

length scales, also demonstrated by 2 linear fits with different slopes in Ref. [2]. In other words, the high-wavenumber contributions of the power spectral density of the surface points dominate the polarization change.

The quadratic relation between d_{EMA} and R_{RMS} was also shown to exist in Ref. [16], where the change in polarization due to the interaction of light with the microscopically rough surface was calculated by second-order Rayleigh–Rice formalism (developed by Franta and Ohlidal [17]) and fitted to the EMA calculations. Furthermore, Yanguas-Gil et al. [18] calculated a small correlation length approximation of the Rayleigh–Rice theory for self-affine surfaces. Such surfaces have R_{RMS} values that scale as L^{α}, were α is the roughness exponent, an additional characteristic parameter originating from the dynamics of roughness growth. In the calculations, a $d_{EMA} \sim R_{RMS}^2/\xi^{\alpha}$ relationship was proven. Similar to the interpretation done in Ref. [18], that the average surface slope (R_{dq}, root mean square average of the local slope, see Ref. [19]) scales as R_{RMS}/ξ^{α}, the d_{EMA} value can be plotted as a function of the product of this R_{dq} and the R_{RMS} value. Fig. 4 reveals a linear correlation for the present study. Excellent linear fit is achieved for $R_{RMS}*R_{dq}$ values smaller than 2 nm. For larger values, downward deviations from the extrapolated line appear, hinting at higher order corrections in the Rayleigh–Rice formalism with, for example, a secondary effect of ξ on d_{EMA} at a unique $R_{RMS}*R_{dq}$ value (see inset in Fig. 4). The linear relationship, mentioned in the many experimental reports [1–7], between R_{RMS} measured by AFM and d_{EMA} measured by ellipsometry can be explained by the fact that the slopes remain constant in most roughening dynamics [1].

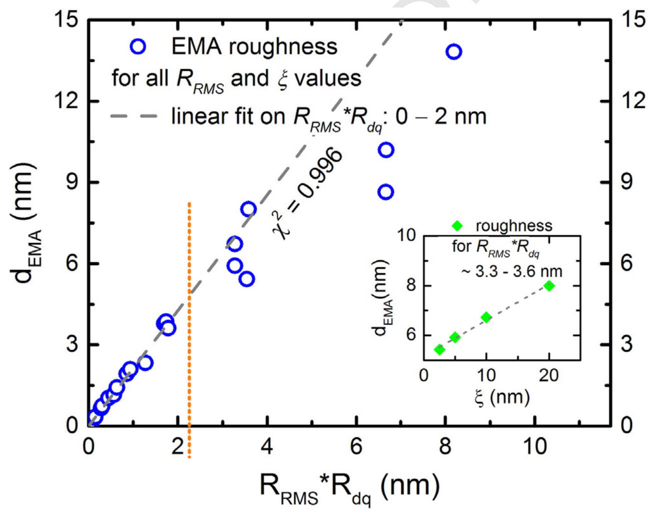

Fig. 4. Correlation between the product of RMS roughness and RMS slope ($R_{RMS}*R_{dq}$) and the thickness of the effective medium roughness (d_{EMA}) with linear fit for abscissa values smaller than 2 nm. The inset shows the secondary effect of correlation length (ξ) on d_{EMA} for points which have an $R_{RMS}*R_{dq}$ value of ~3.4 nm.

4. Conclusions

Finite-element method proves to be a very useful tool to simulate the ellipsometric response of light reflected from microscopic stochastic surface roughness. Not hindered by the sample preparation and the experimental conditions, one can define ideal Gaussian random surfaces with well-defined morphological parameters, such as the RMS roughness and the correlation length in our case. As the effective medium approximation is the most widely used model in ellipsometric evaluations of surface roughness, the present paper focused on the correlation between the fitted EMA thickness and the RMS roughness. A linear relationship between the d_{EMA} and the product of the RMS roughness and the average surface slope has been found for smaller d_{EMA} values, in accordance with the results analytically calculated with Rayleigh–Rice formalism and with the vast experimental measurements reported in previous papers. The deviation from the linear relationship foreshadows further corrections between the relationship of d_{EMA} and the surface morphological parameters.

Acknowledgments

This work was supported by the OTKA grant nos. K81842 K115852, by ENIAC E450EDL project, the Hungarian–French Intergovernmental S&T Cooperation Program TÉT, as well as the M-ERA-NET project no. 117847.

References

[1] A. Yanguas-Gil, H. Wormeester, Relationship between surface morphology and effective medium roughness, in: M. Losurdo, K. Hingerl (Eds.), Ellipsometry at the Nanoscale, Springer, Berlin Heidelberg, Berlin, Heidelberg 2013, pp. 179–202, http://dx.doi.org/10.1007/978-3-642-33956-1.
[2] S.J. Fang, W. Chen, T. Yamanaka, C.R. Helms, Comparison of Si surface roughness measured by atomic force microscopy and ellipsometry, Appl. Phys. Lett. 68 (1996) 2837, http://dx.doi.org/10.1063/1.116341.
[3] P. Petrik, L.P. Biró, M. Fried, T. Lohner, R. Berger, C. Schneider, J. Gyulai, H. Ryssel, Comparative study of surface roughness measured on polysilicon using spectroscopic ellipsometry and atomic force microscopy, Thin Solid Films 315 (1998) 186–191, http://dx.doi.org/10.1016/S0040-6090(97)00349-0.
[4] P. Petrik, T. Lohner, M. Fried, L.P. Biró, N.Q. Khánh, J. Gyulai, W. Lehnert, C. Sneider, H. Ryssel, Ellipsometric study of polycrystalline silicon films prepared by low-pressure chemical vapor deposition, J. Appl. Phys. 87 (2000) 1734, http://dx.doi.org/10.1063/1.372085.
[5] P. Petrik, M. Fried, T. Lohner, R. Berger, L.P. Biró, C. Schneider, J. Gyulai, H. Ryssel, Comparative study of polysilicon-on-oxide using spectroscopic ellipsometry, atomic force microscopy, and transmission electron microscopy, Thin Solid Films 313-314 (1998) 259, http://dx.doi.org/10.1016/S0040-6090(97)00829-8.
[6] H. Fujiwara, J. Koh, P. Rovira, R. Collins, Assessment of effective-medium theories in the analysis of nucleation and microscopic surface roughness evolution for semiconductor thin films, Phys. Rev. B 61 (2000) 10832–10844, http://dx.doi.org/10.1103/PhysRevB.61.10832.
[7] H. Fujiwara, M. Kondo, A. Matsuda, Real-time spectroscopic ellipsometry studies of the nucleation and grain growth processes in microcrystalline silicon thin films, Phys. Rev. B 63 (2001) 115306, http://dx.doi.org/10.1103/PhysRevB.63.115306.
[8] B.A. Sperling, J.R. Abelson, Simultaneous short-range smoothening and global roughening during growth of hydrogenated amorphous silicon films, Appl. Phys. Lett. 85 (2004) 3456–3458, http://dx.doi.org/10.1063/1.1777414.
[9] S. Burger, L. Zschiedrich, J. Pomplun, M. Blome, F. Schmidt, Advanced finite-element methods for design and analysis of nanooptical structures: applications, in: L.-C. Chien, D.J. Broer, V. Chigrinov, T.-H. Yoon (Eds.),Proc. SPIE 2013, p. 864205, http://dx.doi.org/10.1117/12.2001094.
[10] H. Fujiwara, Spectroscopic Ellipsometry: Principles and Applications, Wiley, New York, 2007http://dx.doi.org/10.1002/9780470060193.
[11] R.M.A. Azzam, N.M. Bashara, Ellipsometry and Polarized Light, Elsevier Science B.V., 1987
[12] C.M.M. Herzinger, B. Johs, W.A. McGahan, J.A. Woollam, W. Paulson, Ellipsometric determination of optical constants for silicon and thermally grown silicon dioxide

via a multi-sample, multi-wavelength, multi-angle investigation, J. Appl. Phys. 83 (1998) 3323–3336, http://dx.doi.org/10.1063/1.367101.

[13] D. Bergström, http://www.mysimlabs.com/surface_generation.html2012.

[14] N. Garcia, E. Stoll, Monte Carlo Calculation for electromagnetic-wave scattering from random rough surfaces, Phys. Rev. Lett. 52 (1984) 1798–1801, http://dx.doi.org/10.1103/PhysRevLett.52.1798.

[15] D. Aspnes, J. Theeten, F. Hottier, Investigation of effective-medium models of microscopic surface roughness by spectroscopic ellipsometry, Phys. Rev. B 20 (1979) 3292–3302, http://dx.doi.org/10.1103/PhysRevB.20.3292.

[16] D. Franta, I. Ohlídal, Comparison of effective medium approximation and Rayleigh-Rice theory concerning ellipsometric characterization of rough surfaces, Opt. Commun. 248 (2005) 459–467, http://dx.doi.org/10.1016/j.optcom.2004.12.016.

[17] D. Franta, I. Ohlidal, Ellipsometric parameters and reflectances of thin films with slightly rough boundaries, J. Mod. Opt. 45 (1998) 903–934, http://dx.doi.org/10.1080/095003498151456.

[18] A. Yanguas-Gil, B.a. Sperling, J.R. Abelson, Theory of light scattering from self-affine surfaces: relationship between surface morphology and effective medium roughness, Phys. Rev. B Condens. Matter Mater. Phys. 84 (2011) 1–8, http://dx.doi.org/10.1103/PhysRevB.84.085402.

[19] G. Palasantzas, Static and dynamic aspects of the rms local slope of growing random surfaces, Phys. Rev. E 56 (1997) 1254–1257, http://dx.doi.org/10.1103/PhysRevE.56.1254.

Please cite this article as: B. Fodor, et al., Effective medium approximation of ellipsometric response from random surface roughness simulated by finite-element method, Thin Solid Films (2016), http://dx.doi.org/10.1016/j.tsf.2016.01.054